Journal of Soil Science and Plant Nutrition (2026) 26:7034–7046
https://doi.org/10.1007/s42729-026-03319-0

ORIGINAL PAPER

Linking Carbon fractionation and Mineralization Potential in Young Alder and Oak Trees' Rhizosphere Soil During the Growing Season

Novalia Kusumarini[1,3] · Iseult Lynch[1] · Liam R. Cox[2] · Sami Ullah[1]

Received: 24 November 2025 / Accepted: 30 April 2026 / Published online: 6 May 2026
© The Author(s) under exclusive licence to Sociedad Chilena de la Ciencia del Suelo 2026

Abstract

Predicting soil carbon sequestration after reforesting former farmland requires understanding how tree types and seasons influence fast- and slow-cycling carbon in the rhizosphere. This study investigated the impact of species and seasonal shifts on the distribution and mineralization of labile and stable carbon pools of young forests. We compared a young (~5-year) N_2-fixing alder (*Alnus glutinosa*) with a non-N_2-fixing oak (*Quercus robur*) across the growing season, expecting mineral-associated organic carbon (MAOC) to dominate total soil organic carbon (SOC), and C mineralization potential to peak in spring. We fractionated rhizosphere soils into particulate organic carbon (POC; >53 µm) and MAOC (<53 µm) and measured CO_2 efflux from each fraction to predict C mineralization potential using a Gompertz model. In this young reforested system, MAOC dominated soil carbon pools (>70% of SOC). Most of the soil carbon and nitrogen was stored in the fine fraction than the coarse fraction, highlighting the strong mineral association. The POC/SOC ratio varied with species and season (alder>oak; autumn peak), whereas MAOC/SOC was comparatively invariant. Although MAOC exhibited a larger potentially mineralizable C, POC mineralized>25 times faster per unit C, with autumn consistently highest. Alder soils exhibiting a higher intensity of organic functional group peaks, particularly in the light fraction and POC, and show stronger C=O (carbonyl) signals. Overall, this finding suggests that POC drives the seasonal C mineralization, while MAOC provides the stable backbone of C storage at this newly established forest, potentially enhancing long-term C sequestration from the outset.

Highlights

- Most of the soil C and N are stored in mineral-associated organic matter (MOAM) (<53 µm).
- Partitioning of C and N between MAOM and particulate organic matter (POM) is similar in alder and oak rhizosphere soils.
- Alder soils show a more labile signature with higher POC: MAOC ratios.
- MAOC contains a larger potentially mineralizable C pool, but POC mineralizes much faster per unit C.
- Mineralization rate peaks in spring, particularly in POC.

Keywords Gompertz model · Carbon mineralization rate · Mineral-associated organic carbon (MAOC) · Particulate organic carbon (POC) · FTIR spectroscopic

1 Introduction

Plant roots deliver organic carbon (OC) to soil primarily via rhizodeposition (exudates, mucilage, and sloughed cells) and root litter (Dijkstra et al. 2021). Exudate-derived carbon supplies both fast-cycling particulate organic carbon (POC) and slower-cycling mineral-associated organic carbon (MAOC), and can contribute 2–13 times more C to soil than root litter alone (Sokol and Bradford 2019; Sokol et al. 2019) and become a key factor in the formation of stable

✉ Novalia Kusumarini
novakusuma@ub.ac.id; nxk120@student.bham.ac.uk

✉ Sami Ullah
s.ullah@bham.ac.uk

[1] School of Geography, Earth and Environmental Sciences, University of Birmingham, Birmingham, UK

[2] School of Chemistry, University of Birmingham, Birmingham, UK

[3] Faculty of Agriculture, Universitas Brawijaya, Malang, Indonesia

fractions that represent MAOC that is protected from microbial decomposition (Villarino et al. 2021). In the rhizosphere, these rhizodeposits fuel plant–microbe interactions that not only elevate microbial activity and carbon-use efficiency but can also trigger priming that destabilizes existing soil organic carbon (SOC), accelerating decomposition losses (Jones et al. 2009; Dijkstra et al. 2021). Chemical, physical, and biological processes in the rhizosphere, collectively referred to as the rhizosphere effect, vary significantly among plant species (Massaccesi et al. 2015). Because species differ in exudate quantity and chemical composition, they assemble distinct microbial communities and modulate priming as a nutrient-acquisition strategy (Haldar and Sengupta 2015). For example, in N_2-fixing trees, such as alder, *Alnus glutinosa*, a substantial share of photosynthate supports symbiotic N_2 fixation in root nodules, reducing the tree's reliance on extensive fine-root systems and enabling N acquisition at lower structural C cost (Fisher et al. 2010; Menge et al. 2024; Perkowski et al. 2024). N_2-fixing trees can also promote SOC stabilization and increase the proportion of recalcitrant C by increasing the proportion of MAOC (Wakelin et al. 2021; Ye et al. 2022, 2023; Huang et al. 2025). By contrast, in non-N_2-fixing species such as oak, *Quercus robur*, C allocation is more sensitive to soil N availability (Gill and Finzi 2016; Menge et al. 2024). Nevertheless, over short timescales, OC mineralization, the process by which microorganisms break down organic carbon into simpler inorganic forms, may not differ significantly among species (Hellequin et al. 2021).

Seasonality strongly modulates SOC dynamics, especially the labile, rapidly decomposable C pool (Wang et al. 2022; Gao et al. 2023b; Al-Graiti et al. 2025). Annual shifts in temperature and soil moisture drive microbial respiration, growth, and biomass that regulate the carbon priming effect (CPE) in the rhizosphere and affect the accumulation of SOC (Wu et al. 2021a; Sarkar et al. 2024; Shi et al. 2025). Consistently, higher annual temperatures are associated with increased SOC, POC, and MAOC contents in forest soils, highlighting the critical role of temperature in shaping soil carbon pools (Zhang et al. 2024). Rhizodeposition, particularly root exudation, is also seasonal, and typically peaks during periods of rapid plant growth, when photosynthesis and nutrient demand are high (Chen et al. 2023a; Gao et al. 2024). Field evidence underscores these observations: in a boreal pine forest, rhizosphere C flux in late summer can be sevenfold greater than in early summer. Finally, soil warming can also increase the contribution of microbial residues to mineral-associated C, potentially enhancing C sequestration even as decomposition accelerates (Ding et al. 2019).

Accordingly, understanding rhizosphere C dynamics requires quantifying how C input partitioning between POC and MAOC mediates both C mineralization and stabilization (Lavallee et al. 2020; Chen et al. 2023b). At broader scales, variability in total SOC and its associated physical and chemical fractions in forest soils is driven more strongly by climatic factors than by forest type (Zhang et al. 2024), underscoring the importance of environmental controls on these processes. POC and MAOC fractions differ mechanistically in how they interact with SOC: MAOC is protected from decomposition through association with soil minerals, while POC remains largely unbound and is therefore more accessible to decomposers (Lavallee et al. 2020). MAOC often dominates SOC stocks (~78–86%), serving as the principal long-lived C pool, particularly in forest soil (Chen et al. 2023b; Liu et al. 2025a). Despite its higher stability, MAOC can be destabilized when root exudates dissolve minerals or release bound carbon, enhancing microbial decomposition and carbon loss (Dijkstra et al. 2021; Jilling et al. 2021). By contrast, POC turns over rapidly and is highly sensitive to short-term shifts in temperature, moisture, and substrate supply because it lacks strong physicochemical protection(Lavallee et al. 2020). In short, the balance between C stabilization (in MAOC) and C mineralization (from POC and destabilized MAOC) is central to understanding how rhizosphere processes regulate soil carbon persistence.

Root-derived carbon inputs stimulate OC mineralization by enhancing microbial activity in the rhizosphere, influencing both POC and MAOC fractions (Jilling et al. 2021; Zhang et al. 2022a, 2022b). Root exudates, in particular, drive rapid turnover of the fast-cycling POC pool, which can subsequently contribute to MAOC formation. This microbial stimulation is often reflected in higher soil CO_2 efflux, a commonly used proxy for C mineralization (Liang et al. 2023). Because soil CO_2 emissions integrate the effects of substrate availability and microbial activity, they provide insight into how root inputs regulate soil-carbon cycling (Hui et al. 2020; Song et al. 2022). To capture these dynamics more precisely and to distinguish between short-term responses and longer-term stabilization processes, modeling approaches are often applied to soil CO_2 emission data. The Gompertz model, for example, has been used to estimate the maximum mineralizable C and mineralization rate, reflecting the fact that peak decomposition often occurs in the initial phase of mineralization (Hui et al. 2020; Silva et al. 2023). Such approaches improve our ability to quantify how root-driven microbial processes shape C cycling. Ultimately, understanding CO_2 emission as the product of OC metabolism is essential for assessing the dual role of soils as both sources and sinks of atmospheric CO_2, with direct implications for soil management and climate change mitigation (Gougoulias et al. 2014).

Although soil C dynamics have been widely studied, relatively few studies have compared tree functional traits in

relation to N_2-fixing alder and non-N_2-fixing oak trees. This knowledge gap is particularly pronounced for rhizosphere soils, which are strongly influenced by root exudation, and in young forest systems that still carry legacy effects from previous agricultural use. This study aims to examine how tree species and seasonal variation shape rhizosphere OC dynamics, with a focus on the distribution of C across POC and MAOC fractions, the potential for C mineralization, and the characterization of OC functional groups during the early stages of forest development. We hypothesize that seasonal variation will exert a stronger influence than tree species on CO_2 emissions and C mineralization potential in young forest soils. However, we expect MAOC to consistently account for a higher proportion of total SOC than POC, reflecting MAOC's role as the primary stabilized C pool in the rhizosphere.

2 Materials and Methods

2.1 Study Site and Sampling Method

Soil samples were collected in mid-spring, summer, and autumn of 2024 from a recently established (~5 years) plantation at the Birmingham Institute of Forest Research (BiFoR), Staffordshire, England (52°48′13.2″ N, 2°17′46.1″ W). Sampling was conducted in the rhizosphere by excavating soil directly adjacent to the main tap root and carefully collecting the soil adhering to roots (Wang et al. 2023). The same trees were sampled across all three seasons to ensure consistency. Fresh samples were immediately passed through a 2-mm sieve and stored at 4 °C until subsequent analysis. The soils were classified as silt loam, with a texture of 7.04 ± 0.32% clay, 56.05 ± 1.47% silt, and 36.91 ± 1.75% sand.

2.2 Carbon Fractionation

Soil organic matter fractions were separated into free light fraction (FLF), particulate organic carbon (POC), and mineral-associated organic carbon (MAOC) using a particle size–density fractionation procedure modified from Jilling et al. (2020). Briefly, 20 g of air-dried soil (at ambient laboratory conditions) was dispersed in 50 mL of deionized water (DIW) and shaken at 200 rpm for 18 h. After centrifugation (5000 rpm, 10 min), the floating material collected on a 53 µm sieve was identified as the FLF and oven-dried at 60 °C for 48 h. The remaining soil was resuspended in 25 mL DIW, shaken for 1 h, and sonicated (60 J). The suspension was sieved at 53 µm, with the retained fraction identified as POC and oven-dried (60 °C, 48 h). The < 53 µm fraction was centrifuged (5000 rpm, 35 min), and the resulting pellet was identified as MAOC and dried under the same conditions.

Organic carbon (OC) and nitrogen concentrations of bulk soil and the POC and MAOC fractions were quantified using an elemental analyzer (Vario PYRO cube; Elementar Analysensysteme GmbH, Hanau, Germany). Before analysis, carbonates were removed with 1 M hydrochloric acid (Shi et al. 2024). Briefly, finely ground samples were weighed into centrifuge tubes, and hydrochloric acid was slowly added to minimize bubbling at a soil-to-solution ratio of 1:5. Samples were left to react for 24 h at room temperature, centrifuged (5000 rpm, 10 min), and the supernatant was decanted. The pellet was washed three times with DIW (shaken at 200 rpm for 1 h, followed by centrifugation at 5000 rpm for 10 min) to remove residual acid. The final pellet was transferred to a pre-weighed aluminum foil container and oven-dried at 60 °C for 48 h before elemental analysis.

2.3 Carbon Mineralization Potential

Carbon mineralization potential of each soil fraction (POC and MAOC) was assessed by measuring CO_2 release during short-term incubations under controlled laboratory conditions. Soil samples were adjusted to 45% gravimetric water content, and 1 g of rewetted soil was transferred into 12 mL Exetainer vials (Labco, UK) for headspace gas collection. Samples were pre-incubated at room temperature (~24 °C) inside a cardboard box for 24 h to allow microbial communities to equilibrate. (Butcher et al. 2020). Following pre-incubation, 6 mL of headspace gas was collected at t = 0, 1, 3, 12, 18, 36, 60, and 84 h. Gas sampling was discontinued once no further increase in CO_2 concentration was observed. At each sampling interval, the vials were opened for 20 min to re-equilibrate with ambient air before being resealed. Collected gas samples were transferred into 12 mL Exetainers and diluted with 6 mL of N_2 (two times dilution). Soil moisture was maintained at 45% throughout the incubation period. CO_2 concentrations were quantified using a gas chromatograph (GC; Agilent Technologies, USA) equipped with a flame ionization detector (FID). Final concentrations were corrected for the applied dilution factor.

The cumulative C mineralization potential (CO_2 emission) was estimated using the Gompertz model (Hui et al. 2020) with the following equation:

$$Ct = (A + \mu i) * \exp(-b * \exp(-kt) + et \quad (1)$$

where Ct is the cumulative soil CO_2 emission at time t; A is the asymptotic maximum cumulative CO_2 emission (i.e., the mineralizable C pool size), μi is the random effect associated with replicate i; b is a Gompertz model parameter related to the turning point of the curve; k is an exponent

that indicates the mineralization rate (time $^{-1}$); and *et* is the residual error term at time t.

The net mineralization coefficient (NMC) was calculated based onGuo et al. (2023) from the total C released as CO_2 divided by the TOC in the sample per fraction using the following equation:

$$NMC = \frac{CO_2 - C}{(TOC_{fraction} \times time)} \quad (2)$$

Where *NMC* is the net mineralization coefficient, $CO_2 - C$ is the cumulative carbon released as CO_2 during the incubation period, *TOC* is the total organic carbon content of the corresponding fraction, and t is the time.

2.4 Analysis of the Organic Carbon Functional Groups Using Fourier Transform Infrared (FTIR) Spectroscopy

FTIR spectra of organic carbon in each fraction were acquired from soils that were manually ground to a fine powder. Approximately 1 mg of each sample was vacuum-pressed and analyzed on a PerkinElmer micro-FTIR imaging system to characterize the organic functional groups. Spectra were collected as 16 co-added scans at 4 cm^{-1} spectral resolution over 4000–600 cm^{-1}. Peak positions were detected and band intensities extracted in R using the pracma package and functional groups identified following Table S1.

2.5 Statistical Analysis

Statistical analyses were conducted using RStudio (version 2024.04.2+764; R Core Team 2017). A linear mixed model (LMM) was used to assess the effects of soil sources (alder and oak rhizosphere soil) and seasons on the responses. This analysis was conducted using the lmer function from the lme4 package. Correlations among variables were examined using Spearman correlation tests and R-squared coefficients. Permutational multivariate analysis of variance (PERMANOVA, 999 permutations) was used to determine differences in overall FTIR spectra results. To quantify the effect of oak rhizosphere soil relative to alder, the natural log of the response ratio (lnRR) was calculated as an effect size along with its pooled variance (V) using the following formula:

$$lnRR = ln\left(\frac{Xe}{Xa}\right) \quad (3)$$

$$V = \frac{Se^2}{(Ne + Xe^2)} + \frac{Sa^2}{(Na + Xa^2)} \quad (4)$$

where: Xe and Xa are the mean values of a specific variable in oak and alder soil, respectively; Ne and Na are the sample sizes; and Se and Sa are the standard deviations.

3 Results

3.1 Total Organic Carbon (TOC) and Total Nitrogen (TN) Distribution

Neither tree species nor season had a significant effect on the total carbon and nitrogen pools in the alder rhizosphere ($p>0.05$; Table S2), indicating that overall C and N contents remained relatively stable over the short term. However, when partitioned by fraction size, the finer fraction contained substantially higher nutrient concentrations, with organic carbon (OC) and nitrogen (N) levels being 17-fold and 20-fold greater, respectively, compared to the coarser fraction size across all soil sources and seasons ($p<0.001$; Fig. 1A and B). Although differences between rhizosphere soil of alder and oak were not statistically significant, the response ratio (lnRR) of alder rhizosphere soils tended to hold slightly larger C (lnRR = −0.214; Fig. 5) and N pools (lnRR = −0.211) in coarse fractions, while in fine fractions, oak soil tended to have slightly higher C pool (lnRR = 0.007; Fig. 5). The C: N ratio, in contrast, showed a slight increase in coarser particles (Fig. 1C); however, this effect was negligible and not statistically significant ($p=0.611$).

3.2 Carbon Fractionation Distribution

In both alder and oak rhizosphere soils, most OC was contributed by the MAOC, accounting for more than 70% of SOC across all seasons, while POC contributed comparatively little, reaching a maximum of only 16% of SOC in alder soils ($p<0.001$; Fig. 2A). Despite the dominance of MAOC in carbon storage, the physically coarser fraction linked to POC represented about 70% of the soil mass, whereas the finer fraction accounted for only 25% on average; the remaining proportion was attributed to the light fraction, likely derived from decomposed litter (Fig. 2B). Comparison between alder and oak rhizosphere soils revealed no significant differences in this young forest system; however, alder soil tended to have a slightly higher POC contribution to SOC than oak (lnRR = −0.220; Fig. 5) but lower MAOC contribution to SOC (lnRR = 0.066; Fig. 5). The POC/MAOC ratio, used as an indicator of carbon stabilization, was 34% higher in alder rhizosphere soils than in oak ($p<0.001$, Table S2; Fig. 2C), particularly in spring, suggesting a greater proportion of labile carbon in alder compared to oak. This pattern indicates that alder supports more dynamic C cycling than oak.

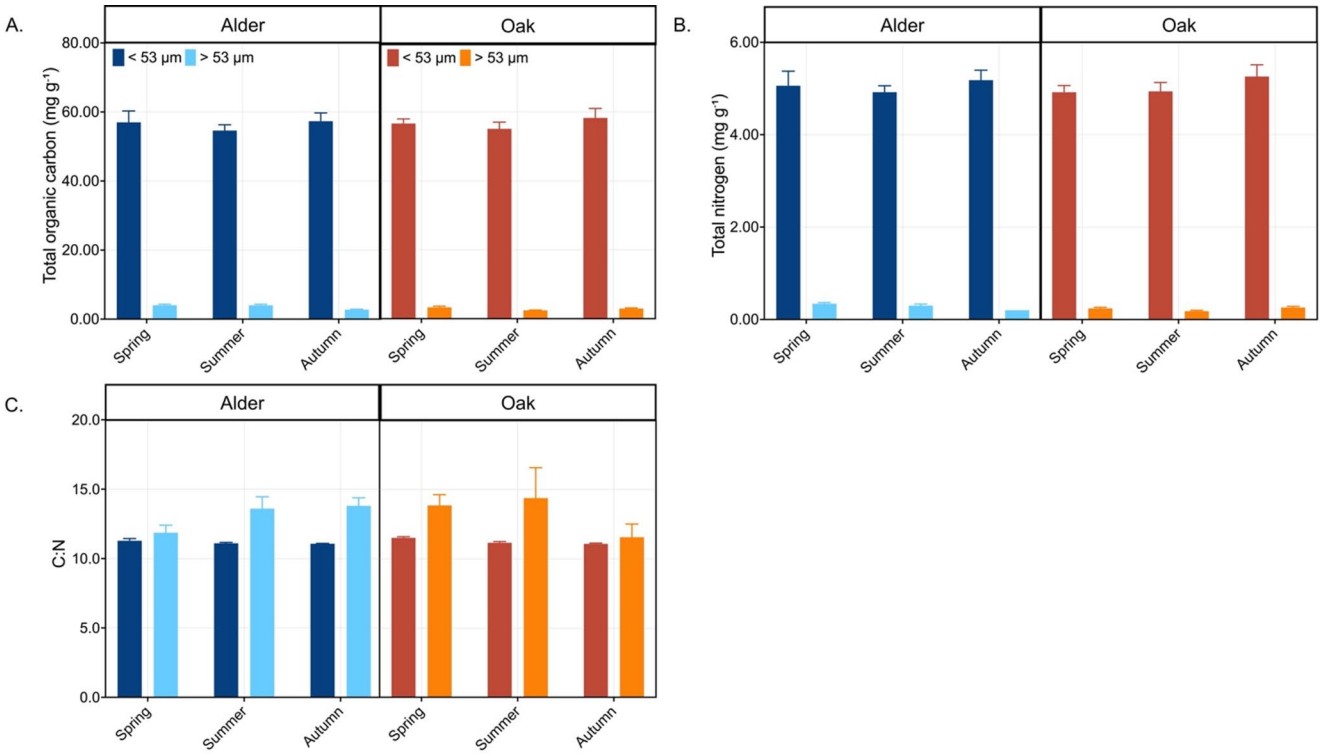


Fig. 1 (**A**) Total organic carbon (TOC), (**B**) Total nitrogen (TN), and (**C**) C: N ratio in particulate (>53 µm) and mineral-associated (<53 µm) soil fractions. Values are means ± SE ($n = 5$)

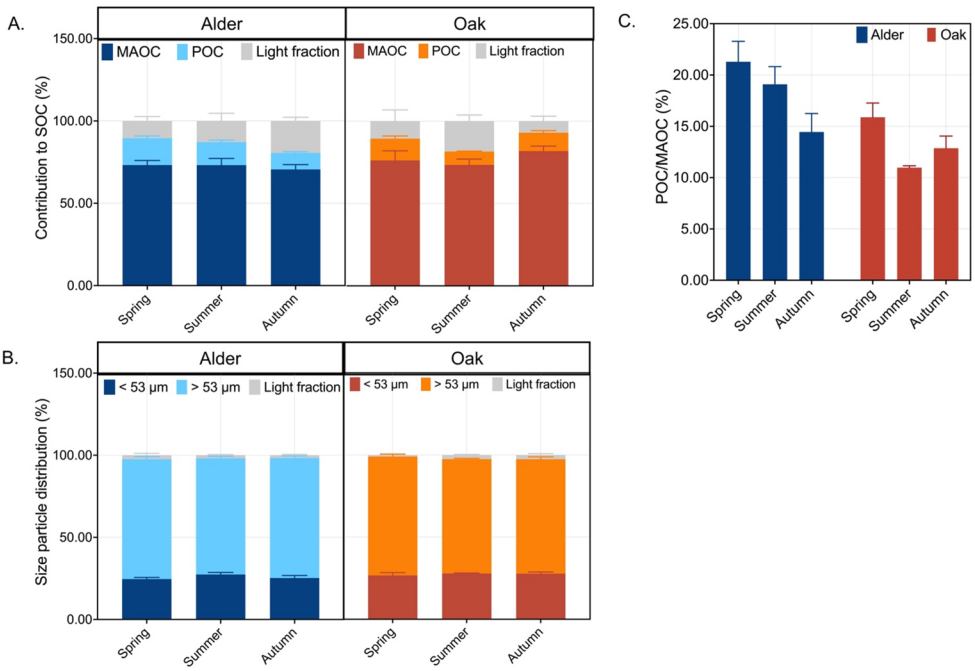


Fig. 2 (**A**) Distribution of total organic carbon (TOC) content of Particulate Organic Carbon (POC), Mineral-Associated Organic Carbon (MAOC) in Soil Organic Carbon (SOC); (**B**) Particle size distribution to SOC, and (**C**) POC to MAOC ratio in the soil rhizosphere of alder and oak trees across the growing season. Values are means ± SE ($n = 5$)

3.3 Cumulative Soil CO_2 Production

Over the short term (84 h), neither soil source (alder vs. oak) nor season affected cumulative CO_2 emissions ($p > 0.05$; Table S2). In contrast, soil fraction did ($p = 0.048$; Table S2), where MAOC exhibited greater cumulative C mineralization than POC (Fig. 3A). The larger cumulative CO_2 emission from MAOC likely reflects its larger TOC pool. Upon a longer incubation period, additional CO_2 emissions became negligible,

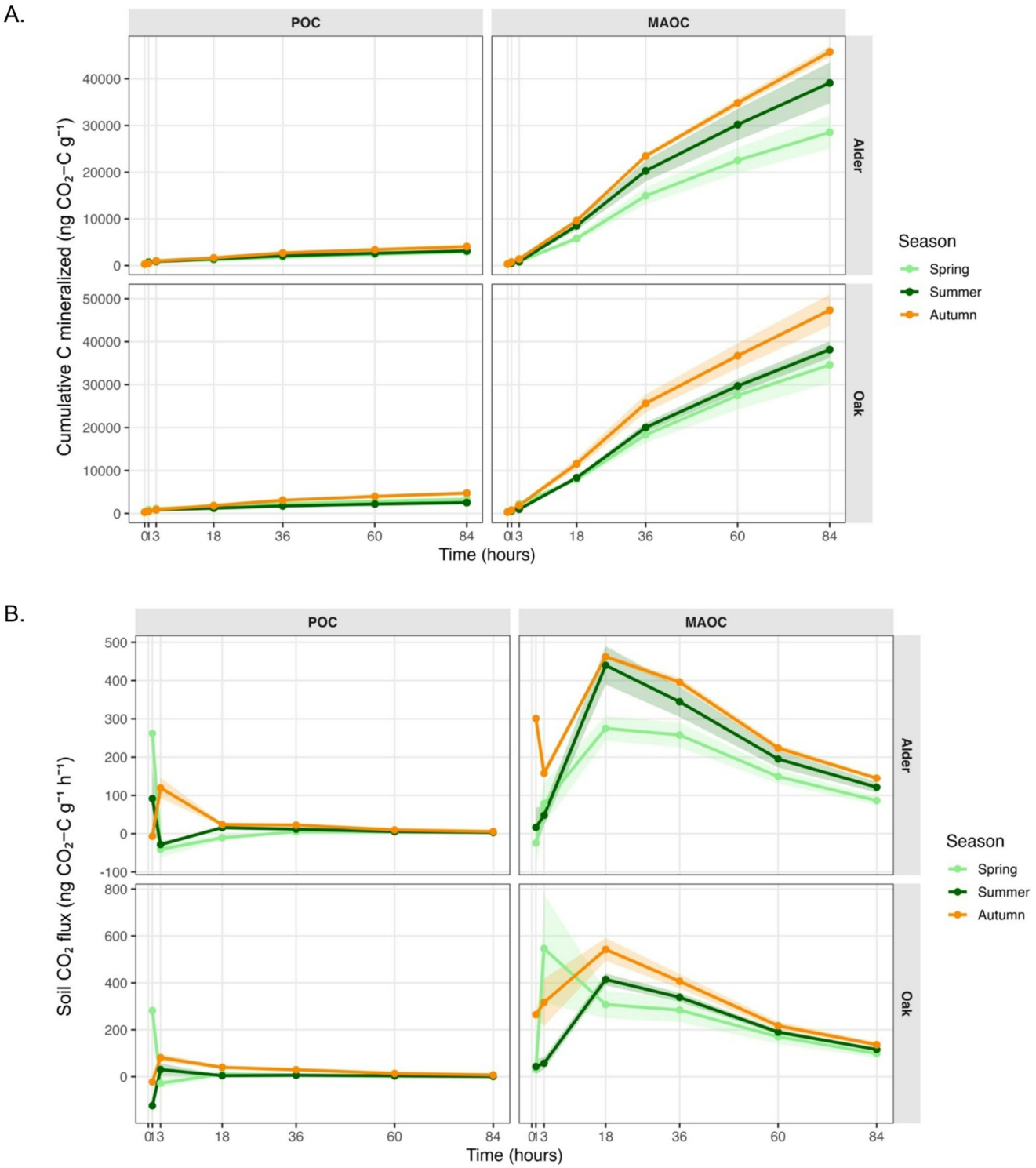


Fig. 3 (**A**) Cumulative CO_2–C mineralized and (**B**) CO_2 flux during an 84-h incubation for Particulate Organic Carbon (POC) and Mineral-Associated Organic Carbon (MAOC) fractions from alder and oak rhizosphere soils across the growing season. Shaded area are means ± SE

likely due to a rapid decline in microbial activity as readily available substrates were depleted in the closed system. This pattern is mirrored in the CO_2 flux, which peaked during the first 18 h, particularly in MAOC, and declined sharply thereafter (Fig. 3B). Across seasons, spring showed higher early-time fluxes than summer or autumn ($p < 0.001$; Table S2), but seasonal differences were not evident after 60 h.

Using a Gompertz model, we estimated potential cumulative CO_2 emission (A), the shape parameter (b), and the rate parameter (k). In this young forest system, species (alder vs. oak) did not affect A ($p>0.05$, Table S2), whereas season and soil fraction did ($p<0.001$). The highest C mineralization potential occurred in autumn, exceeding the lowest season (spring) by 75% in POC and 48% in MAOC (Table 1). Across species, oak tended to have lower C mineralization potential in the POC fraction (lnRR = −0.018) but higher C mineralization potential in the MAOC fraction (lnRR = 0.042) than alder, but these differences were not statistically significant ($p>0.05$; Fig. 5). MAOC showed 15-fold greater C mineralization potential than POC. Consistent with a pool-size mechanism, it is correlated positively with TOC in both fractions (POC: $r=0.94$, $p=0.01$; MAOC: $r=0.64$, $p=0.08$). Regarding the shape model parameter (b), species and season had no effect ($p>0.05$), but SOM fraction did ($p<0.001$). MAOC showed a 2.75-fold greater b value than POC, indicating that MAOC has a longer lag time before the CO_2 emission increases.

Consistent with the results for C mineralization potential, the mineralization rate did not differ by species (alder vs. oak, $p>0.05$) but did vary by season ($p=0.002$) and soil fraction ($p=0.037$). Spring showed the highest mineralization rate across treatments. In MAOC, which was 4 times higher in alder and 3 times higher in oak relative to autumn (the season with the lowest CO_2 mineralization), matching the steeper early increase in cumulative CO_2. In POC, the spring increase in mineralization rate was larger in oak (2.14×) than in alder (1.08×). Averaged across seasons and species, MAOC exhibited a roughly double mineralization rate than POC. Notably, the mineralization rate was not significantly correlated with TOC, implying that the rate of mineralization reflects substrate reactivity and microbial activity rather than pool size.

The net mineralization coefficient (NMC) was significantly ($p<0.001$; Table S2) higher in POC than in MAOC, being 38-fold higher in POC than in MAOC across all seasons and soil sources (Fig. 4), indicating that this fraction

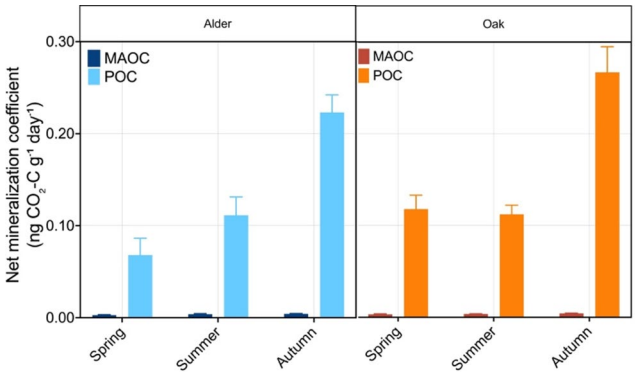


Fig. 4 Net carbon mineralization coefficient (NMC) in particulate organic carbon (POC) and mineral-associated organic carbon (MAOC) fractions of alder and oak soils. Values are means ± SE ($n=5$)

contributed most to C mineralization. No significant differences were detected between alder and oak soils ($p>0.05$), although oak tended to show slightly higher POC NMC values (lnRR = 0.164) than MAOC NMC (lnRR = 0.024; Fig. 5). Seasonal effects were pronounced ($p<0.001$), with the highest NMC observed in autumn, particularly in POC, which was 110% greater than the lowest value recorded in spring (Fig. 4). Across fractions, NMC was strongly correlated with TOC and TN ($r=-0.83$, $p<0.001$), CO_2 emission ($r=0.93$, $p<0.001$), and potential cumulative CO_2 emission ($r=0.53$, $p<0.001$). Together, these results indicate that POC contains more labile carbon and mineralizes more rapidly than the more stable carbon in MAOC. Although tree species did not significantly influence C mineralization potential in this young forest system, the consistent trend of slightly higher values in oak soils suggests species effects may become more pronounced over time.

3.4 Functional Groups

FTIR spectroscopic analysis identified three major functional groups: C=O (carbonyl) stretching, most abundant

Table 1 Gompertz parameter estimates for cumulative CO_2–C mineralization in POC and MAOC from alder and oak rhizosphere soils. Values are mean ± SE ($n=5$)

Soil source	Season	Fraction	A (ng CO_2-C g^{-1})[1]	B[2]	k (h^{-1})[3]
Alder	Spring	POC	710.77 ± 67.17	0.16 ± 0.05	5.21 ± 1.84
Alder	Summer	POC	676.98 ± 43.31	0.15 ± 0.04	4.62 ± 1.45
Alder	Autumn	POC	1083.45 ± 86.21	0.31 + 0.08	4.81 ± 1.67
Oak	Spring	POC	630.82 ± 21.98	0.00 ± 0.00	11.29 ± 0.17
Oak	Summer	POC	537.40 ± 28.23	0.14 ± 0.05	5.55 ± 1.94
Oak	Autumn	POC	1258.90 ± 111.57	0.27 ± 0.05	3.60 ± 0.32
Alder	Spring	MAOC	9326.34 ± 933.82	0.61 ± 0.03	21.20 ± 5.78
Alder	Summer	MAOC	13350.50 ± 476.61	0.44 ± 0.02	10.33 ± 4.53
Alder	Autumn	MAOC	13425.53 ± 512.20	0.48 ± 0.03	4.21 + 0.06
Oak	Spring	MAOC	9749.33 ± 1381.99	0.42 ± 0.09	18.23 ± 7.24
Oak	Summer	MAOC	11937.69 ± 574.66	0.49 ± 0.02	4.32 + 0.06
Oak	Autumn	MAOC	14888.90 ± 835.57	0.36 ± 0.06	4.61 ± 0.29

[1]A represents the mineralizable C pool size

[2] b is a Gompertz model parameter related to the turning point of the curve

[3] K is an exponent that indicates the mineralization rate

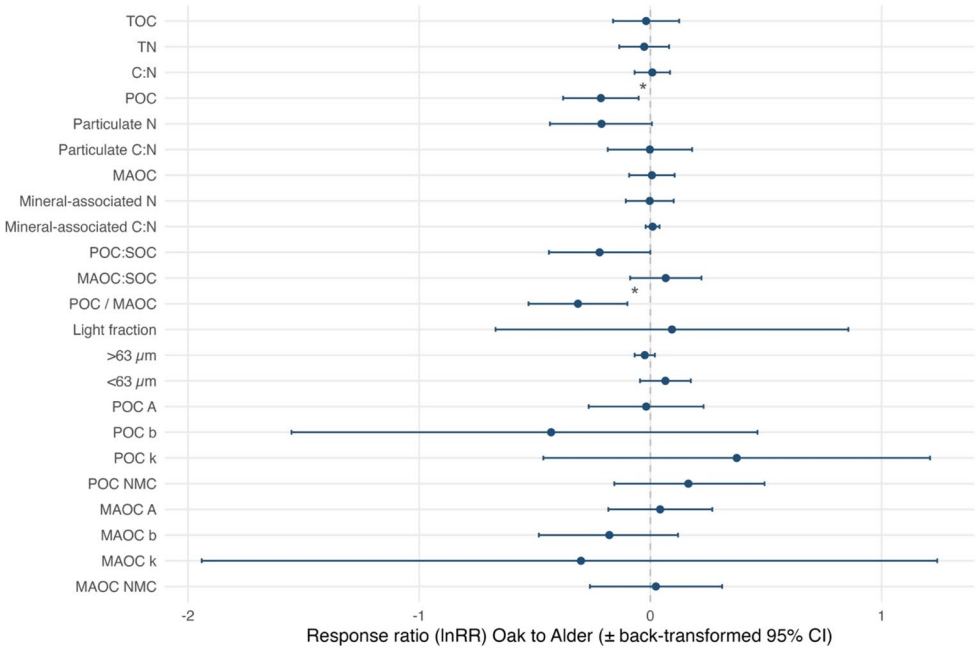


Fig. 5 Species effect sizes are expressed as log response ratios, oak to alder for soil carbon pools, nitrogen pools, stoichiometric ratios, particle-size fractions, and kinetic parameters. Points show estimated ratios from the fitted models, and bars denote 95% confidence intervals. The dashed vertical line (ratio = 0) represents no species effect. Ratios < 0 indicate greater values under alder, whereas ratios > 0 indicate greater values under oak. Asterisks (*) indicate statistically significant differences between species after multiple comparison correction (adjusted $p < 0.05$)

in the light fraction (LF) and POC; N-H bending; and C–H (aliphatic) stretching (Fig. S1). The aliphatic group was not detected in the MAOC of either alder or oak soils (Fig. 6A). Alder soils displayed slightly greater diversity and stronger intensities of functional groups compared to oak. Across the soil fractions, the fine fraction (MAOC) contained the least diverse set of functional groups, with only carbonyl signals present in alder soils and none in oak soils, whereas

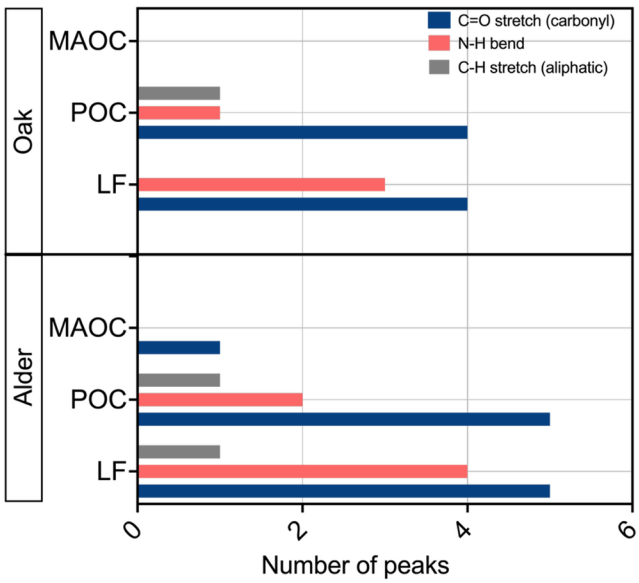


Fig. 6 Functional groups in Mineral Associated Organic Carbon (MAOC), Particulate Organic Carbon (POC), and Light Fraction (LF) fractions of alder and oak rhizosphere soils across growing seasons. Note that LF was included in the FTIR characterization only and was not part of the carbon mineralization experiment

the coarse fraction (POC) and LF exhibited a broader range of functional groups.

4 Discussion

In the early stages of forest development, the accumulation of carbon (C) and nitrogen (N) in the rhizosphere does not appear to be species-specific. Our results showed that in both alder and oak soils, the fine particle-size fraction (< 53 µm), operationally corresponding to mineral-associated organic matter (MAOM), contained substantially higher amounts of soil C and N than the coarse fraction (> 53 µm), defined as particulate organic matter (POM). Specifically, carbon concentrations in the fine fraction were 14–23 times higher than in the coarse fraction, while nitrogen concentrations were 15–27 times higher. This predominance of MAOM likely reflects both the legacy effects of previous land use and the limited carbon inputs from roots and litter in young stands. As trees grow and belowground production intensifies, carbon inputs are expected to increase, gradually enhancing soil carbon stocks, particularly in the particulate (POM) fraction (Sariyildiz et al. 2016; Hou et al. 2020; Ma et al. 2024). This observation indicates that most soil C and soil N are mineral-protected, enhancing their stability, as MAOM is physically formed through the binding of dissolved organic matter or microbial necromass and by-products to minerals and metal colloids (Dijkstra et al. 2021; Manzoni and Cotrufo 2024). Consistent with this, MAOC accounted for over 70% of SOC, highlighting the dominance of stable carbon in the rhizosphere and suggesting a high carbon sink

potential during early forest development; this is particularly critical for forest management, given that the soil C sink capacity typically declines with forest age (Leng et al. 2024). At this early stage of forest development, species did not significantly influence OC accumulation in either the MAOC or POC fractions. Nevertheless, alder soils contained slightly higher C and N in the POM fraction, while oak soils had somewhat greater C in the MAOM fraction (Fig. 5). This pattern likely reflects the legacy of prior agricultural land use, which left MAOC undersaturated; thus, new C inputs were preferentially stabilized in MAOC rather than accumulating in labile pools, minimizing species differences (Georgiou et al. 2022; Six et al. 2024). The slightly higher MAOC formation in oak may be explained by greater inputs of labile C from root exudates, as shown by lower C: N ratio) that stimulate microbial activity (Kusumarini 2026). This is consistent with previous findings that MAOC formation is preferentially promoted by high-quality C from root exudation (Villarino et al. 2021), microbial biomass, and microbial activity (Sokol and Bradford 2019; Gao et al. 2023a; Liang et al. 2023; Cheng et al. 2025), whereas POC accumulation is more closely linked to litter decomposition (Cheng et al. 2025). Moreover, C:N stoichiometry is a key regulator of MAOC formation; for instance, the C: N ratios of plant litter and microbial biomass, the primary precursors of MAOC, determine the efficiency of carbon transformation and its subsequent stabilization in mineral-associated pools (Liu and Chen 2024). Over time, distinct species are expected to exert clearer effects on C and N accumulation, particularly in the MAOC fraction, thereby enhancing long-term C stability and sequestration potential. Both POC, MAOC, and total SOC typically increase during forest growth, though the magnitude of that increase varies among forest types; for instance, coniferous forests often show lower increases compared to broad-leaved forests (Cheng et al. 2025). Our findings suggest that in young, reforested soils, legacy effects currently outweigh species effects, but root-driven MAOC formation will determine the trajectory of long-term C and N sequestration.

In contrast to the relatively stable MAOC contribution to SOC, the POC/SOC ratio was strongly affected by both species and season. This result is expected because POC is closely tied to plant fragmentation and fine-root quality, and is readily occluded within soil aggregates, making it highly responsive to short-term environmental variation (Lavallee et al. 2020; Gao et al. 2023a). Consequently, temperature and moisture shifts can rapidly alter POC dynamics (Hansen et al. 2024). In our study, POC contributed least to SOC in autumn, particularly in alder soil. Cooler temperatures and reduced belowground inputs in autumn likely lower the incorporation and occlusion of fresh plant fragments, diminishing POC's relative share (Hansen et al. 2024). By contrast, spring showed the highest POC contribution in both species, consistent with greater biological activity, root growth, and aggregate formation under warmer, moister conditions (Rawlik et al. 2022; Chen et al. 2025). Furthermore, Autumn litterfall accumulates over winter under reduced microbial activity, and subsequent spring warming stimulates its decomposition, leading to a transient peak in POC, whereas higher summer temperatures further enhance microbial turnover and drive a seasonal decline in POC (Zhang et al. 2014; Wang et al. 2022). Comparing species, alder soils had a higher proportion of POC than oak. We attribute this result to the slightly lower quality of belowground C fluxes under alder (root exudate C: N ratio), but also more variable metabolomic compounds (Kusumarini 2026), which generate more particulate inputs and rapid occlusion before complete decomposition, thereby elevating the POC share of SOC. Although alder is typically associated with higher-quality litter, belowground carbon allocation patterns may differ between species and are not necessarily reflected by aboveground litter traits. More broadly, organic matter quality helps govern partitioning between particulate and mineral-associated pools. Recalcitrant inputs tend to persist as POC, whereas high-quality, labile inputs more readily form MAOC (Cotrufo et al. 2013). Consistent with our results, a study from the central Himalayas reported that Nepalese alder (*Alnus nepalensis*) contributes more SOC than co-occurring oaks (Shankar and Garkoti 2024). Together, these mechanisms explain why POC distribution is sensitive to species traits and seasonal dynamics, whereas MAOC remains comparatively buffered.

Consistent with the higher POC under alder, the POC/MAOC ratio was also species-specific, indicating that alder supplies richer, faster-cycling C inputs (Li et al. 2022; Six et al. 2002) and is associated with greater mineralization potential (Lavallee et al. 2020) than oak. Numerous studies show that N_2-fixing trees produce higher-quality litter that stimulates soil microbial biomass and extracellular enzyme activities (Liu et al. 2025b; Ma et al. 2023; Wedderburn and Carter 1999). In contrast, high-quality rhizodeposition (e.g., root exudates), as observed for oak, more efficiently forms MAOC (Villarino et al. 2021), consistent with the lower POC/MAOC ratio determined in oak soils. Moreover, oak's frequent association with EM tends to promote carbon storage and organic-matter stabilization (Averill et al. 2014; Liu et al. 2023). Together, these patterns suggest that alder, via higher-quality litter inputs, accelerates carbon cycling, whereas oak, via higher-quality rhizodeposits and EM associations, favors the formation of stabilized and mineral-protected C, an insight with clear implications for future forest management and C sequestration as a nature-based solution for climate change mitigation.

Although MAOC is typically viewed as the more persistent pool, it is not uniformly slow cycling (Sokol et al. 2022). Our study showed that MAOC yielded higher cumulative CO_2 emissions than POC for both alder and oak. This pattern is consistent with rhizosphere processes that both stabilize and destabilize OC, which can be promoted by root-derived inputs (Dijkstra et al. 2021; Zhang et al. 2022a). Low-molecular-weight exudates such as oxalic acid can displace or dissolve mineral-bound OC via ligand exchange and mineral alteration, releasing protected C that is then rapidly respired, as priming-like C loss, rather than directly fueling microbial growth (Keiluweit et al. 2015; Jilling et al. 2021). Because MAOM is relatively nutrient-dense and microbially processed, desorbed MAOC tends to be quickly assimilated and decomposed, elevating microbial respiration (Lavallee et al. 2020). By contrast, POC is physically unprotected, more readily available, but its quality for decomposers is less consistent than that of MAOC (Lavallee et al. 2020). Labile C inputs also accelerate turnover of mineral-protected OC via competitive sorption and related processes, producing an early respiration burst from MAOC (Kalbitz et al. 2005). These mechanisms explain our Gompertz fits, where a larger potential mineralizable C (A value) for MAOC reflects a larger mineralizable pool, amplified by its much greater pool size in our soils (>90% of total C), which means a bigger C substrate, as C substrate has a positive correlation with MAOC decomposition (Zhang et al. 2022a, 2022b). When desorption-driven bursts dominate, MAOC can also show a steeper mineralization rate constant (k) and a shorter lag time (b), due to rapid respiration of newly released C compounds (Kalbitz et al. 2005). In sum, the greater cumulative CO_2 emission from MAOC may reflect desorption-driven respiration and large pool size, rather than inherently higher per-C lability, so it still serves as the long-term, mineral-protected C sink.

Despite the larger mineralizable C potential (A) in MAOC, the net mineralization coefficient (NMC) rate was over 25 times higher in POC, and this difference was season-driven, with the highest rates in autumn, but not species-dependent. Mechanistically, POC is dominated by plant fragments with short residence times and high microbial accessibility, so it decomposes rapidly and responds strongly to short-term environmental variation (Lavallee et al. 2020). This labile pool fuels microbial activity and can facilitate early forest succession(Sun et al. 2025). By contrast, MAOC's larger potential mineralizable C (A) value mainly reflects its greater pool size, but when expressed per unit C, POC mineralizes faster because it is less protected and less stable (Lavallee et al. 2020). Consistent with our results, multiple studies report higher POC mineralization and greater short-term temperature sensitivity for POC than for MAOC (Rocci et al. 2021; Li et al. 2024). Seasonally, autumn promotes mineralization through fresh litter inputs from leaf senescence (Naldini et al. 2021) and the reactivation of microbes upon soil rewetting after summer dryness (Zhang et al. 2022b), with moderate temperatures and improved moisture further enhancing decomposition. In contrast, MAOC NMC remains comparatively stable across seasons, reflecting its lower environmental sensitivity and role as the most persistent, mineral-protected fraction of SOC (Rocci et al. 2021; Zhang et al. 2025). Taken together, MAOC sets the long-term storage, but POC sets the seasonal pulse of CO_2 emission spiking in autumn, suggesting that both fractions have critical functions in forest development.

Functional-group composition was driven more by species than season (Fig. 6B), with alder soils exhibiting a broader suite of detectable bands in FTIR spectra than oak. The spectra were characterized by the C=O stretch (carbonyl), which was assigned to carboxylic acids, esters, amide/protein, and microbial residues, which were most pronounced in the light fraction and POC and were present in alder MAOC but not in oak MAOC. This pattern aligns with a larger labile OC pool under alder, consistent with its higher POC: MAOC ratio and with reports linking stronger carbonyl signals to more easily decomposable pools (Obeng 2023; Zheng et al. 2021). It also fits the view that carbonyl-rich features in mineral fractions reflect microbial necromass that readily associates with minerals (Liang et al. 2019). We also observed overlapping aromatic C=C signals (lignin, phenolics, humic substances) and N–H bending (proteins/peptides, lignin derivatives, humic substances), again concentrated in the light fraction/POC. The aromatic component is commonly interpreted as more recalcitrant organic C (Zheng et al. 2021). By contrast, only weak C–H (aliphatic) stretches, attributed to cellulose, hemicellulose, and polysaccharides, appeared in POC, supporting the idea that POC comprises accumulated, more decomposed particulate organic material rather than fresh, waxy or carbohydrate-rich inputs (Tavanti et al. 2023). Overall, POC/light fractions displayed greater chemical diversity than MAOC, which was enriched in more microbially processed, low-molecular-weight, and more stable C (Lavallee et al. 2020). Finally, the greater variability, especially in carbonyl groups in alder soil, suggests a larger, more labile OC pool, which may compromise aggregate stability relative to that in oak soil (Wu et al. 2021b). This finding indeed points to the fact that oaks may enable more stable soil C over time with relevance for C sequestration.

5 Conclusion

In this young reforested cropland, soil organic carbon (SOC) was dominated by the fine fraction (MAOC; <53 μm), with only a minor proportion in the coarse particulate fraction (POC and other coarse materials). This distribution was consistent across species (alder, oak) and seasons (spring,

summer, autumn). The co-location of most soil C and N in the fine fraction suggests strong mineral protection against microbial decomposition. Despite the dominance of MAOC within SOC, alder soils exhibited a higher POC: MAOC ratio than oak soils, reflecting a more labile organic carbon signature. Incubation data further indicated that although MAOC contained a larger potentially mineralizable C pool due to its size, POC mineralized substantially faster on a per-unit-C basis. Seasonally, net C mineralization peaked in autumn, with the strongest seasonal response in the POC fraction, while the highest rate constant occurred in spring. FTIR spectroscopic analysis revealed species differences: alder soils displayed greater functional-group intensity and stronger C=O (carbonyl) signals, especially in the light and POC fractions, whereas oak soils showed fewer and less diverse functional features, particularly in MAOC. Collectively, these findings indicate that POC drives the seasonal dynamics of C mineralization, whereas MAOC provides the stable foundation for long-term C storage in this newly established forest. Promoting the transformation of carbonyl-rich residues from POC into MAOC will be key to strengthening long-term soil C sequestration as the system matures, for example by maintaining continuous organic inputs and stable microclimatic conditions that favor microbial processing and mineral stabilization.

Supplementary Information The online version contains supplementary material available at https://doi.org/10.1007/s42729-026-03319-0.

Acknowledgements The authors would like to thank the Technical Team at BIFoR-FACE, who maintain and operate the experimental site, making this experiment possible. Additionally, the authors thank the Norbury Park Estate for allowing access to the plantation for research.

Authors Contribution Novalia Kusumarini: Writing original draft, visualization, methodology, investigation, formal analysis, data curation, and conceptualization. Iseult lynch: Writing (review and editing), supervision, and funding acquisition. Liam R. Cox: Writing (review and editing), supervision. Sami Ullah: Writing (review and editing), supervision, conceptualization, methodology, and funding acquisition.

Funding This work was funded by the Indonesian Endowment Fund for Education (LPDP; Ref. Number LOG-2494/LPDP.3/2024).

Declarations

Competing Interests The authors declare that they have no known competing financial interests or personal relationships that could have appeared to influence the work reported in this paper.

References

Al-Graiti T, Szalai Z, Ujházy N et al (2025) Seasonal changes of soil organic matter composition in separate carbon pools of a cultivated Chernozem: The role of crops and fertilization. Geoderma Reg 40. https://doi.org/10.1016/j.geodrs.2025.e00943

Averill C, Turner BL, Finzi AC (2014) Mycorrhiza-mediated competition between plants and decomposers drives soil carbon storage. Nature 505:543–545. https://doi.org/10.1038/nature12901

Butcher KR, Nasto MK, Norton JM, Stark JM (2020) Physical mechanisms for soil moisture effects on microbial carbon-use efficiency in a sandy loam soil in the western United States. Soil Biol Biochem 150. https://doi.org/10.1016/j.soilbio.2020.107969

Cheng H, Su Y, Huang Z et al (2025) Distribution, characteristics, and importance of particulate and mineral-associated organic carbon in China forest: a meta-analysis. PeerJ 13. https://doi.org/10.7717/peerj.19189

Chen M, Yao X, Cheng H et al (2023a) Changes in Chinese fir plantations root exudation strategies seasonally and as tree age. Ecol Manag 545. https://doi.org/10.1016/j.foreco.2023.121239

Chen R, Yin L, Wang X et al (2023b) Mineral-associated organic carbon predicts the variations in microbial biomass and specific enzyme activities in a subtropical forest. Geoderma 439. https://doi.org/10.1016/j.geoderma.2023.116671

Chen Z, Arif M, Tian M (2025) Elevation and seasonality modulate the leaf decomposition rates and nutrient flux of diverse species and species richness in karst river systems across China. Front Plant Sci 16. https://doi.org/10.3389/fpls.2025.1543011

Cotrufo MF, Wallenstein MD, Boot CM et al (2013) The Microbial Efficiency-Matrix Stabilization (MEMS) framework integrates plant litter decomposition with soil organic matter stabilization: Do labile plant inputs form stable soil organic matter? Glob Chang Biol 19:988–995. https://doi.org/10.1111/gcb.12113

Dijkstra FA, Zhu B, Cheng W (2021) Root effects on soil organic carbon: a double-edged sword. New Phytol 230:60–65

Ding X, Chen S, Zhang B et al (2019) Warming increases microbial residue contribution to soil organic carbon in an alpine meadow. Soil Biol Biochem 135:13–19. https://doi.org/10.1016/j.soilbio.2019.04.004

Fisher JB, Sitch S, Malhi Y et al (2010) Carbon cost of plant nitrogen acquisition: A mechanistic, globally applicable model of plant nitrogen uptake, retranslocation, and fixation. Global Biogeochem Cycles 24. https://doi.org/10.1029/2009gb003621

Gao F, Cui X, Chen M, Sang Y (2023a) Forest Conversion Changes Soil Particulate Organic Carbon and Mineral-Associated Organic Carbon via Plant Inputs and Microbial Processes. Forests 14. https://doi.org/10.3390/f14061234

Gao T, Song X, Ren Y et al (2023b) Effects of seasonal changes on the carbon dynamics in mixed coniferous forests. PLoS One 18. https://doi.org/10.1371/journal.pone.0267365

Gao Y, Wang H, Yang F et al (2024) Relationships between root exudation and root morphological and architectural traits vary with growing season. Tree Physiol 44. https://doi.org/10.1093/treephys/tpad118

Georgiou K, Jackson RB, Vindušková O et al (2022) Global stocks and capacity of mineral-associated soil organic carbon. Nat Commun 13. https://doi.org/10.1038/s41467-022-31540-9

Gill AL, Finzi AC (2016) Belowground carbon flux links biogeochemical cycles and resource-use efficiency at the global scale. Ecol Lett 19:1419–1428

Gougoulias C, Clark JM, Shaw LJ (2014) The role of soil microbes in the global carbon cycle: Tracking the below-ground microbial processing of plant-derived carbon for manipulating carbon dynamics in agricultural systems. J Sci Food Agric 94:2362–2371

Guo J, Xiong W, Qiu J, Wang G (2023) Linking soil organic carbon mineralization to soil physicochemical properties and bacterial alpha diversity at different depths following land use changes. Ecol Process 12. https://doi.org/10.1186/s13717-023-00450-z

Haldar S, Sengupta S (2015) Plant-microbe Cross-talk in the Rhizosphere: Insight and Biotechnological Potential. Open Microbiol J 31:1–7. https://doi.org/10.2174/1874285801509010001

Hansen PM, Even R, King AE et al (2024) Distinct, direct and climate-mediated environmental controls on global particulate and mineral-associated organic carbon storage. Glob Chang Biol 30. https://doi.org/10.1111/gcb.17080

Hellequin E, Binet F, Klarzynski O et al (2021) Shaping of soil microbial communities by plants does not translate into specific legacy effects on organic carbon mineralization. Soil Biol Biochem 163. https://doi.org/10.1016/j.soilbio.2021.108449

Hou G, Delang CO, Lu X, Gao L (2020) A meta-analysis of changes in soil organic carbon stocks after afforestation with deciduous broadleaved, sempervirent broadleaved, and conifer tree species. Ann Sci 77. https://doi.org/10.1007/s13595-020-00997-3

Huang N, He HY, Fan R et al (2025) Planting of nitrogen-fixing shrubs promote soil carbon sequestration by increasing mineral-associated organic fraction. Geoderma 457. https://doi.org/10.1016/j.geoderma.2025.117282

Hui D, Porter W, Phillips JR et al (2020) Phosphorus rather than nitrogen enhances CO2 emissions in tropical forest soils: Evidence from a laboratory incubation study. Eur J Soil Sci 71:495–510. https://doi.org/10.1111/ejss.12885

Jilling A, Kane D, Williams A et al (2020) Rapid and distinct responses of particulate and mineral-associated organic nitrogen to conservation tillage and cover crops. Geoderma 359. https://doi.org/10.1016/j.geoderma.2019.114001

Jilling A, Keiluweit M, Gutknecht JLM, Grandy AS (2021) Priming mechanisms providing plants and microbes access to mineral-associated organic matter. Soil Biol Biochem 158. https://doi.org/10.1016/j.soilbio.2021.108265

Jones DL, Nguyen C, Finlay RD (2009) Carbon flow in the rhizosphere: Carbon trading at the soil-root interface. Plant Soil 321:5–33

Kalbitz K, Schwesig D, Rethemeyer J, Matzner E (2005) Stabilization of dissolved organic matter by sorption to the mineral soil. Soil Biol Biochem 37:1319–1331. https://doi.org/10.1016/j.soilbio.2004.11.028

Keiluweit M, Bougoure JJ, Nico PS et al (2015) Mineral protection of soil carbon counteracted by root exudates. Nat Clim Chang 5:588–595. https://doi.org/10.1038/nclimate2580

Kusumarini N (2026) From Rhizosphere to Forest Restoration: How Species and Season-Specific Root Exudates Regulate Soil Nutrient Transformation in Young Reforested Plantation. University of Birmingham

Lavallee JM, Soong JL, Cotrufo MF (2020) Conceptualizing soil organic matter into particulate and mineral-associated forms to address global change in the 21st century. Glob Chang Biol 26:261–273. https://doi.org/10.1111/gcb.14859

Leng Y, Li W, Ciais P et al (2024) Forest aging limits future carbon sink in China. One Earth 7:822–834. https://doi.org/10.1016/j.oneear.2024.04.011

Liang C, Amelung W, Lehmann J, Kästner M (2019) Quantitative assessment of microbial necromass contribution to soil organic matter. Glob Chang Biol 25:3578–3590. https://doi.org/10.1111/gcb.14781

Liang G, Stark J, Waring BG (2023) Mineral reactivity determines root effects on soil organic carbon. Nat Commun 14. https://doi.org/10.1038/s41467-023-40768-y

Li J, He L, Wang J et al (2024) Responses of particulate and mineral-associated organic carbon to temperature changes and their mineral protection mechanisms: A soil translocation experiment. Sci Total Environ 948. https://doi.org/10.1016/j.scitotenv.2024.174689

Li J, Shangguan Z, Deng L (2022) Free particulate organic carbon plays critical roles in carbon accumulations during grassland succession since grazing exclusion. Soil Tillage Res 220. https://doi.org/10.1016/j.still.2022.105380

Liu J, Chen J (2024) Developing an ecological stoichiometry-based framework for tracing the sources of soil organic matter. Glob Chang Biol 30:e17384. https://doi.org/10.1111/gcb.17384

Liu L, Gunina A, Zhang F et al (2023) Fungal necromass increases soil aggregation and organic matter chemical stability under improved cropland management and natural restoration. Sci Total Environ 858. https://doi.org/10.1016/j.scitotenv.2022.159953

Liu Y, Huang Y, Ndzelu BS, Hou R (2025a) Carbon saturation level regulates the stability of mineral-associated organic carbon in forest soils. Catena (Amst) 259. https://doi.org/10.1016/j.catena.2025.109391

Liu Y, Li Q, Tian H et al (2025b) Nitrogen-fixing tree species enhance the positive effects of tree species richness on soil organic carbon sequestration by increasing fine root phosphorus loss. Catena (Amst) 254. https://doi.org/10.1016/j.catena.2025.108927

Ma F, Liu Y, Qi Y et al (2024) Tree age affects carbon sequestration potential via altering soil bacterial community composition and function. Front Microbiol 15. https://doi.org/10.3389/fmicb.2024.1379409

Ma J, Luan J, Wang H et al (2023) Nitrogen-fixing tree species rather than tree species diversity shape soil nematode communities in subtropical plantations. Geoderma 436. https://doi.org/10.1016/j.geoderma.2023.116561

Manzoni S, Cotrufo MF (2024) Mechanisms of soil organic carbon and nitrogen stabilization in mineral-associated organic matter - insights from modeling in phase space. Biogeosciences 21:4077–4098. https://doi.org/10.5194/bg-21-4077-2024

Massaccesi L, Benucci GMN, Gigliotti G et al (2015) Rhizosphere effect of three plant species of environment under periglacial conditions (Majella Massif, central Italy). Soil Biol Biochem 89:184–195. https://doi.org/10.1016/j.soilbio.2015.07.010

Menge DNL, Wolf AA, Funk JL et al (2024) Nitrogen fixation and fertilization have similar effects on biomass allocation in nitrogen-fixing plants. Ecol Evol 14. https://doi.org/10.1002/ece3.70309

Naldini MB, Pérez Harguindeguy N, Kowaljow E (2021) Soil carbon release enhanced by increased litter input in a degraded semi-arid forest soil. J Arid Environ 186. https://doi.org/10.1016/j.jaridenv.2020.104400

Obeng AS, Dunne J, Giltrap M et al (2023) Soil organic matter carbon chemistry signatures, hydrophobicity and humification index following land use change in temperate peat soils. Heliyon 9. https://doi.org/10.1016/j.heliyon.2023.e19347

Perkowski EA, Terrones J, German HL, Smith NG (2024) Symbiotic nitrogen fixation reduces belowground biomass carbon costs of nitrogen acquisition under low, but not high, nitrogen availability. AoB Plants 16. https://doi.org/10.1093/aobpla/plae051

Rawlik K, Kasprowicz M, Nowiński M, Jagodziński AM (2022) The afterlife of herbaceous plant species: A litter decomposition experiment in a temperate oak-hornbeam forest. Ecol Manage 507. https://doi.org/10.1016/j.foreco.2022.120008

R Core Team (2017) R: a language and environment for statistical computing. https://www.r-project.org

Rocci KS, Lavallee JM, Stewart CE, Cotrufo MF (2021) Soil organic carbon response to global environmental change depends on its distribution between mineral-associated and particulate organic matter: a meta-analysis. Sci Total Environ 793. https://doi.org/10.1016/j.scitotenv.2021.148569

Sariyildiz T, Savaci G, Kravkaz IS (2016) Effects of tree species, stand age and land-use change on soil carbon and nitrogen stock rates in northwestern Turkey. IForest 9:165–170. https://doi.org/10.3832/ifor1567-008

Sarkar S, Das DK, Singh A et al (2024) Seasonal variations in soil characteristics control microbial respiration and carbon use under tree plantations in the middle gangetic region. Heliyon 10. https://doi.org/10.1016/j.heliyon.2024.e35593

Shankar A, Garkoti SC (2024) Influence of forest types on soil physicochemical and biological characteristics of associated agroecosystems in the central Himalaya. Sci Total Environ 906. https://doi.org/10.1016/j.scitotenv.2023.167731

Shi J, Gong J, Ding M et al (2025) Soil phosphorus availability regulates ecosystem carbon dynamics during the growing season of a typical temperate grassland in inner Mongolia, China. J Arid Environ 230. https://doi.org/10.1016/j.jaridenv.2025.105432

Shi J, Lv J, Peng Y et al (2024) Mechanisms controlling the stability and sequestration of mineral associated organic carbon upon erosion and deposition. Catena (Amst) 242. https://doi.org/10.1016/j.catena.2024.108119

Silva EM, Campos Frühauf A, Menezes da Silva É et al (2023) Sigmoid models in the description of CO_2 evolved from legumes in the soil. Revista Agrogeoambiental e20231776. https://doi.org/10.18406/2316-1817v15nunico20231776

Six J, Conant RT, Paul EA, Paustian K (2002) Stabilization mechanisms of soil organic matter: Implications for C-saturation of soils. Plant Soil 241:155–176. https://doi.org/10.1023/A:1016125726789

Six J, Doetterl S, Laub M et al (2024) The six rights of how and when to test for soil C saturation. SOIL 10:275–279. https://doi.org/10.5194/soil-10-275-2024

Sokol NW, Bradford MA (2019) Microbial formation of stable soil carbon is more efficient from belowground than aboveground input. Nat Geosci 12:46–53. https://doi.org/10.1038/s41561-018-0258-6

Sokol NW, Kuebbing SE, Karlsen-Ayala E, Bradford MA (2019) Evidence for the primacy of living root inputs, not root or shoot litter, in forming soil organic carbon. New Phytol 221:233–246. https://doi.org/10.1111/nph.15361

Sokol NW, Whalen ED, Jilling A et al (2022) Global distribution, formation and fate of mineral-associated soil organic matter under a changing climate: A trait-based perspective. Funct Ecol 36:1411–1429. https://doi.org/10.1111/1365-2435.14040

Song Y, Cheng X, Song C et al (2022) Soil CO2 and N2O emissions and microbial abundances altered by temperature rise and nitrogen addition in active-layer soils of permafrost peatland. Front Microbiol 13. https://doi.org/10.3389/fmicb.2022.1093487

Sun H, Sun F, Deng X et al (2025) Unfolding the Roles of Particulate- and Mineral-Associated Organic Carbon in Soil Microbial Communities. Forests 16. https://doi.org/10.3390/f16010027

Tavanti RFR, Liñares ML, Soares MB et al (2023) Macro-scale spatial modeling reveals the role of soil organic matter quality in CO2 emissions. Geoderma Reg 34. https://doi.org/10.1016/j.geodrs.2023.e00690

Villarino SH, Pinto P, Jackson RB, Piñeiro G (2021) Plant rhizodeposition: A key factor for soil organic matter formation in stable fractions. Sci Adv 7:3176–3190. https://doi.org/10.1126/sciadv.abd317

Wakelin SA, Matson A, Wigley K et al (2021) High Maintenance of Rhizosphere Soil C and N Equilibrium Regardless of Plant Species or Species Traits. Front Soil Sci 1. https://doi.org/10.3389/fsoil.2021.762510

Wang L, Sun Y, Li J et al (2023) Rhizosphere soil nutrients and bacterial community diversity of four broad-leaved trees planted under Chinese fir stands with different stocking density levels. Front For Glob Change 6–2023. https://doi.org/10.3389/ffgc.2023.1135692

Wang X, Sheng L, Li Y et al (2022) Soil labile organic carbon indicating seasonal dynamics of soil organic carbon in northeast peatland. Ecol Indic 138. https://doi.org/10.1016/j.ecolind.2022.108847

Wedderburn ME, Carter J (1999) Litter decomposition by four functional tree types for use in silvopastoral systems. Soil Biol Biochem 31:455–461. https://doi.org/10.1016/S0038-0717(98)00151-5

Wu J, Wang H, Li G et al (2021a) Vertical and seasonal changes in soil carbon pools to vegetation degradation in a wet meadow on the Qinghai-Tibet Plateau. Sci Rep 11. https://doi.org/10.1038/s41598-021-90543-6

Wu M, Pang D, Chen L et al (2021b) Chemical composition of soil organic carbon and aggregate stability along an elevation gradient in Helan Mountains, northwest China. Ecol Indic 131. https://doi.org/10.1016/j.ecolind.2021.108228

Ye X, Luan J, Wang H et al (2022) Tree species richness and N-fixing tree species enhance the chemical stability of soil organic carbon in subtropical plantations. Soil Biol Biochem 174. https://doi.org/10.1016/j.soilbio.2022.108828

Ye Y, Wang H, Luan J et al (2023) Nitrogen-fixing tree species modulate species richness effects on soil aggregate-associated organic carbon fractions. Ecol Manag 546. https://doi.org/10.1016/j.foreco.2023.121315

Zhang F, Chen X, Yao S et al (2022a) Responses of soil mineral-associated and particulate organic carbon to carbon input: A meta-analysis. Sci Total Environ 829. https://doi.org/10.1016/j.scitotenv.2022.154626

Zhang H, Yuan W, Dong W, Liu S (2014) Seasonal patterns of litterfall in forest ecosystem worldwide. Ecol Complex 20:240–247. https://doi.org/10.1016/j.ecocom.2014.01.003

Zhang Y, Guo X, Chen L et al (2024) Global pattern of organic carbon pools in forest soils. Glob Chang Biol 30. https://doi.org/10.1111/gcb.17386

Zhang Y, Li X, Liu X et al (2022b) Effects of Drying and Rewetting Cycles on Carbon Dioxide Emissions and Soil Microbial Communities. Forests 13. https://doi.org/10.3390/f13111916

Zhang Z, Gao H, Gao X et al (2025) Short-term warming supports mineral-associated carbon accrual in abandoned croplands. Nat Commun 16. https://doi.org/10.1038/s41467-024-55765-y

Zheng S, Zhang J, Chi F et al (2021) Response of the chemical structure of soil organic carbon to modes of maize straw return. Sci Rep 11. https://doi.org/10.1038/s41598-021-84697-6

Publisher's Note Springer Nature remains neutral with regard to jurisdictional claims in published maps and institutional affiliations.

Springer Nature or its licensor (e.g. a society or other partner) holds exclusive rights to this article under a publishing agreement with the author(s) or other rightsholder(s); author self-archiving of the accepted manuscript version of this article is solely governed by the terms of such publishing agreement and applicable law.